Effect of temperature on the structure and electrochemical performance of LiFePO$_4$-based composite prepared by microwave chemical vapor deposition

X.R. Zeng [a,b,*], F. Deng [c], J.Z. Zou [a,b]

[a] College of Materials Science and Engineering, Shenzhen University, Shenzhen 518060, China
[b] Shenzhen Key Laboratory of Special Functional Materials, Shenzhen 518060, China
[c] School of Materials Science and Engineering, Northwestern Polytechnical University, Xi'an 710072, China

ARTICLE INFO

ABSTRACT

LiFePO$_4$-based composite cathode materials have been synthesized by a rapid microwave chemical vapor deposition method within 10 min at temperatures as low as 550 °C. The samples prepared at different temperatures have been characterized by X-ray diffraction, field emission scanning electron microscope, energy dispersive X-ray spectroscopy, high resolution transmission electron microscopy and electrochemical measurements in lithium cells. Results show that the composite prepared at 650 °C exhibits the best electrochemical properties, with the discharge capacity as high as 122.7 mAh g^{-1} at 5 C and the charge transfer resistance as low as 80 Ω. This can mainly be attributed to the formation of a three-dimensional conductive network provided by vapor-grown carbon fiber, pyrolytic carbon film and graphite. The synthesis and processing approach presented here offer a simple and high-efficiency method to obtain high-performance LiFePO$_4$ cathode materials.

1. Introduction

Lithium ion battery technology introduced by Sony in 1991 has played a key role in the portable electronics revolution, and the technology is now pursued for vehicle applications. Cobalt-oxide-based materials as cathode in these battery systems have the safety concerns arising from the chemical instability at deep charge [1,2], while spinel LiMn$_2$O$_4$ suffers from severe capacity fade at elevated temperatures [3,4]. Recognizing this, oxides with polyanions like $(XO_4)^{2-}$ (X = S, Mo, and W) were initiated as lithium insertion/extraction hosts since the covalently bonded groups like $(SO_4)^{2-}$ can lower the redox energies of chemically more stable couples like Fe$^{2+/3+}$ through inductive effect and increase the cell voltage [5]. Following this, LiFePO$_4$ (LFP) crystallizing in the olivine structure was identified by Padhi et al. in 1997 as a cathode material [6].

LFP has received much attention owing to its relative lack of toxicity, the low cost and the safety imparted by the covalently bonded PO$_4$ groups. It also has a high lithium intercalation voltage of 3.4 V compared with lithium metal and a high theoretical capacity of 170 mAh g^{-1} [7,8]. However, the major issue with LFP is its low lithium ion and electronic conductivities [9,10]. While the

one-dimensional chains formed by the edge-shared LiO$_6$ octahedra lead to poor lithium ion conductivity, the lack of mixed valency due to the little solubility between LFP and FePO$_4$ and the localized Fe^{2+} or Fe^{3+} lead to low electronic conductivity. Therefore, many efforts have been considerable in recent years to overcome its limitations by cationic doping [11,12], decreasing the particle size [13,14], and coating with electronically conducting agents [15,16].

Up to now, a variety of synthesis procedures have been developed to prepare LFP materials, involving solid-state reactions [17], the sol–gel process [14,18], the hydrothermal synthesis [12,19,20], the solvothermal method [21], mechanical activation [22], coprecipitation [23], the template method [24], the spray technology [25] and the microwave synthesis [26]. The majority of the above synthesis methods require high annealing temperatures, long annealing time or several grinding steps. Among these methods, microwave synthesis was first adopted by Higuchi et al. [26] in 2003 to obtain LFP. Microwave can ensure uniform and fast heating through a self-heating process based on direct microwave energy absorption by the materials [27].

Carbon materials have been reported as ideal conductive fillers in battery systems because of their high electrical and good corrosion resistance in many electrolytes [28,29]. Vapor-grown carbon fiber (VGCF), as a typical representative of carbon materials, has been characterized in terms of the highly preferred orientation of their graphitic basal planes parallel to the fiber axis, with an annular ring texture in the cross section. This structure gives rise to excellent mechanical properties, very high electrical and thermal

* Corresponding author. Tel.: +86 755 26557459; fax: +86 755 26536239.
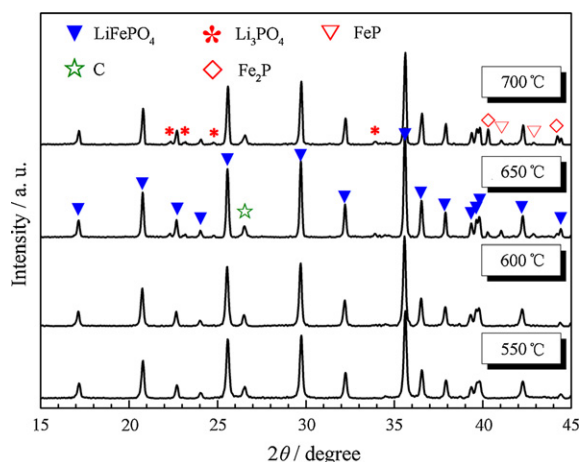E-mail addresses: zengxier@szu.edu.cn (X.R. Zeng), fdeng80@yahoo.com.cn (F. Deng).

Fig. 1. XRD profiles of the samples prepared at different temperatures by MCVD process.

conductivity, and a high graphitizability of the fibers [30]. Chen et al. reported that the first discharge capacity of VGCF enhanced LiFePO$_4$-based composite was more than two times of that without VGCF [31]. Nevertheless, ball milling, the most widely used method to introduce carbon fibers in the mixing process [32,33], could inevitably increase their contact resistance and is difficult to ensure homogeny and dipersity in the eletrodes.

Microwave pyrolysis chemical vapor deposition (MCVD) has ever been developed to obtain VGCF in our previous studies [34–36]. We present here this novel technique to prepare LiFePO$_4$-based composite. A three-dimensional conductive network composed of VGCF, pyrolytic carbon film and graphite can be formed in one step through this process. The effect of temperature on the structure and electrochemical performance of LiFePO$_4$-based composite was studied in detail.

2. Experimental

2.1. Synthesis

The LiFePO$_4$-based composite samples were prepared by a MCVD method. Firstly the starting materials, FeC$_2$O$_4$·2H$_2$O, NH$_4$H$_2$PO$_4$, and LiOH·H$_2$O in stoichiometric amount, were dispersed into acetone, ground with 4.1 wt.% (compared to the LFP to be synthesized) graphite (TIMCAL, TIMREX KS-6) in a ball mill at 300 rpm for 6 h, and then dried under vacuum at 120 °C for 12 h. The as-dried samples were placed in a self-designed quartz reactor installed in the MCVD cavity. After the cavity was filled with argon, the MCVD equipment was operated at 2.45 GHz, with an output power of 800 W. When the temperature reached the setting value (550 °C, 600 °C, 650 °C and 700 °C), propylene with a flow of 90 sccm was put into the quartz reactor for 10 min. Then the MCVD equipment was closed and the samples were cooled naturally to the room temperature.

2.2. Structural, chemical, and physical characterizations

The X-ray powder diffraction (XRD, D8 ADVANCE, Bruker AXS) with Cu Kα radiation was used to identify the phases. Field emission scanning electron microscope (FESEM, S-4800, HITACHI) and energy dispersive X-ray spectroscopy (EDS, EDAX) were used to analyze the morphology and elementary component, respectively. High resolution transmission electron microscopy (HRTEM, JEM-2100F) and selected area diffraction (SAD) were used to analyze the nanostructure of the samples. The amount of carbon in the LiFePO$_4$-based composite samples was determined by a dissolution method using hydrochloric acid as the solvent.

2.3. Electrochemical characterization

The cathodes containing 95 wt.% as-prepared and 5 wt.% polyvinylidene fluoride (PVDF) were prepared by spreading slurry in N-methylpyrrolidone (NMP) onto aluminum foil current collectors and allowing them to dry. 2032 size coin cells were assembled in an argon-filled glove box, using lithium as a counter electrode and 1 M solution of LiPF$_6$ in ethylene carbonate/dimethyl carbonate (EC/DMC) 1:1. Charge–discharge tests were performed using an Arbin Instrument (BT2000) at 25 °C. The electrochemical impedance spectroscopy (EIS) was measured with a frequency response analyzer (Solatron 1260) interfaced with a potentio-galvanostat (Solatron 1287). The alternating current signal applied to the cells was 10 mV in a frequency range from 10^5 Hz to 10^{-2} Hz.

3. Results and discussion

Fig. 1 shows XRD profiles of the samples prepared at different temperatures by MCVD process. All composites synthesized below 650 °C can be indexed to orthorhombic LFP (JCPDS: 83-2092) and rhombohedral graphite-3R (JCPDS: 26-1079). The diffraction peaks of graphite are mainly resulted from the graphite mixed in the raw materials. Minor impurities of Li$_3$PO$_4$, FeP and Fe$_2$P were detected when the preparation temperature was up to 700 °C. According to previous reports, sintering above 800 °C is necessary to obtain single phase LFP [17]. However, our experiments have shown that the single olivine phase can form at much lower temperatures (~550 °C).
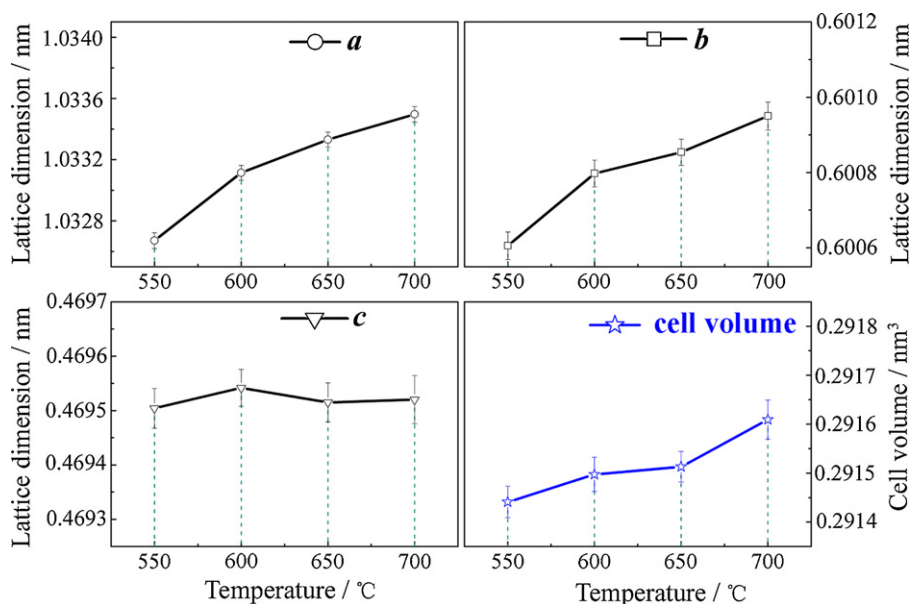

Fig. 2. Influence of the synthesis temperature on rhombic cell volume and lattice parameters of different samples.
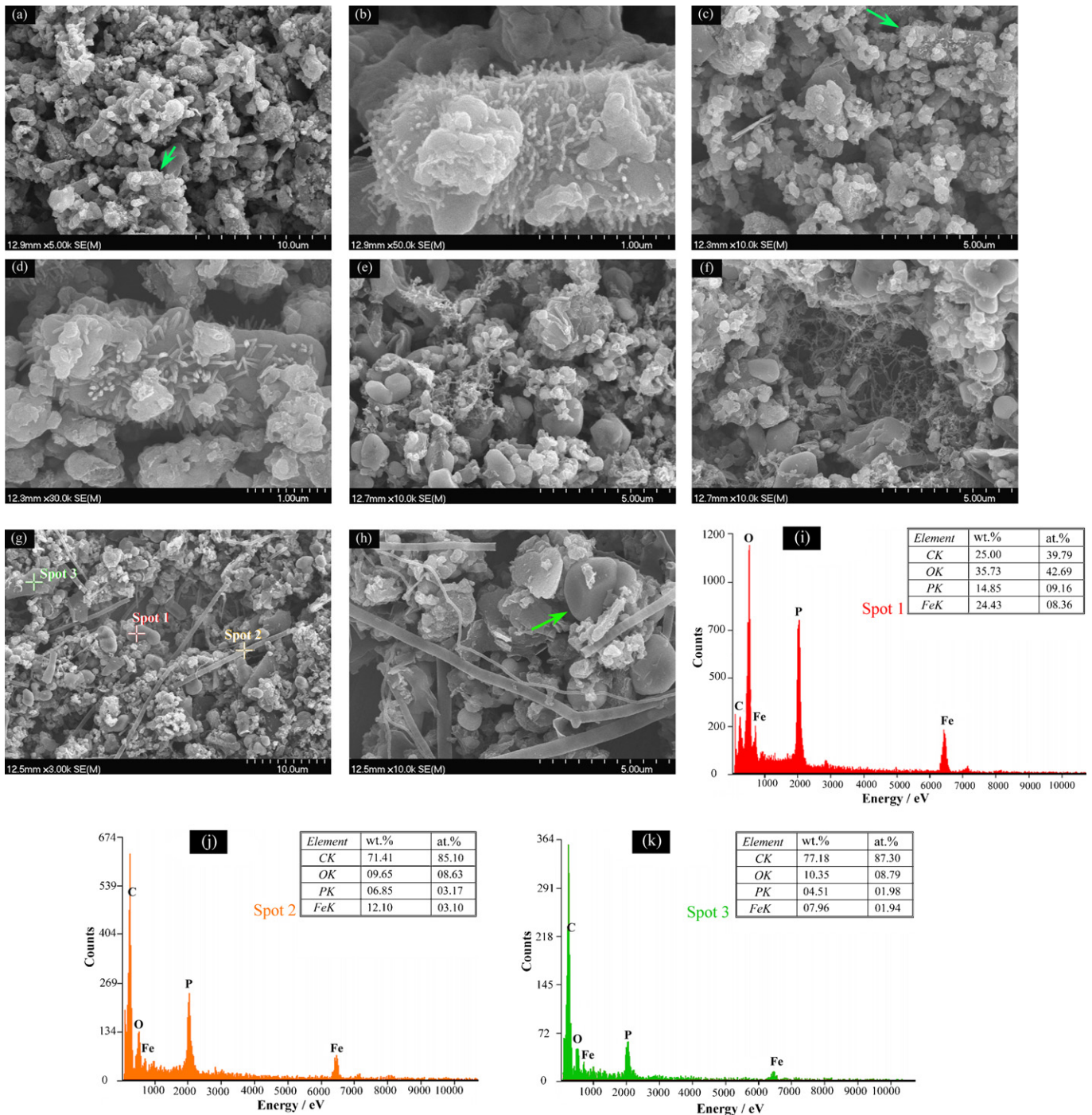
Fig. 3. FESEM morphology and EDS analyses of the samples prepared at different temperatures. (a) 550 °C, (b) higher magnification of (a), (c) 600 °C, (d) higher magnification of (c), (e) 650 °C, (f) the morphology of (e) after dispersed with absolute alcohol, (g) 700 °C, (h) higher magnification of (g), (i) EDS analysis of Spot 1, (j) EDS analysis of Spot 2 and (k) EDS analysis of Spot 3.

In Fig. 2, the volume of the rhombic unit cell and the lattice parameters of the different samples are plotted versus the preparation temperature. The cell volume and the lattice parameters a and b increase with the increased synthesis temperature, whereas the lattice parameter c is almost unaffected. Obviously, there is an expansion of the crystal structure within the crystallographic a–b plane for an increased temperature. This result may indicate the existence of an unidentified stoichiometric or structural deviation from the ideal olivine type LFP, which depends on the synthesis temperature [13].

Fig. 3 shows the FESEM morphology and EDS analyses of the samples prepared at different temperatures. The composite obtained at 550 °C was composed of irregularly shaped LFP (~300 nm), flaky graphite, and needle-like carbon fibers (Fig. 3a). Most carbon fibers grew vertically to the surface of the particles, which formed a radial structure close to the sea-urchin (Fig. 3b). With the temperature increasing from 600 °C to 650 °C, the mean size of LFP particles increased from 500 nm to 800 nm and their shape generally evolved into the ball (Fig. 3c and e). The diameter and the length of the carbon fibers obtained at 600 °C are
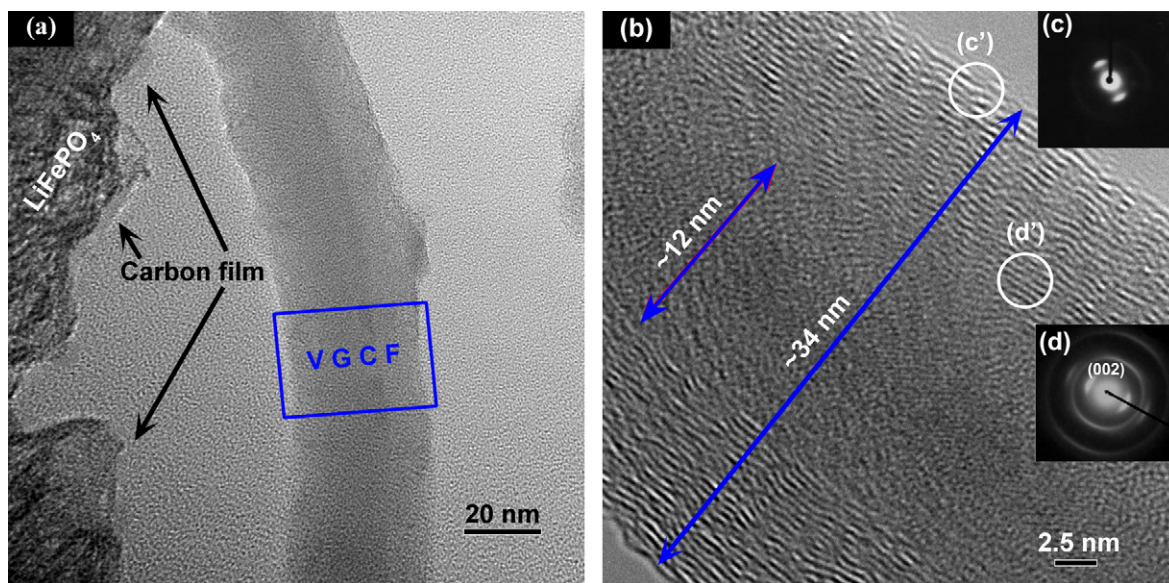
Fig. 4. (a) The HRTEM image of the sample prepared at 550 °C, (b) the magnified image of the rectangular area of VGCF shown in (a), (c) is the SAD pattern of the encircled region of (c′) and (d) is the SAD pattern of the encircled region of (d′).

obviously bigger than those got at 550 °C (Fig. 3d). A carbon–fiber network was formed when the temperature was up to 650 °C. It could be observed more distinctly by FESEM after the composite was dispersed with absolute alcohol (Fig. 3f). The particle shape of LFP synthesize at 700 °C was almost globular and the size of individual particles was up to ~2.5 μm because of abnormal grain growth (Fig. 3g and h). The carbon fibers grew into a branching or bamboo-structured shape and they interlaced with each other in the composite.

HRTEM was used to analyze the nanostructure of the sample prepared at 550 °C (Fig. 4). A carbon film was observed on the surface of LFP grain. The carbon film may result from the pyrolysis and deposition of propylene, which was also reported by Belharouak

et al. [15]. In addition, the carbon fibers exhibited a typical VGCF structure (Fig. 4c and d) that had a highly preferred orientation of their graphitic basal planes parallel to the fiber axis [28]. Endo et al. has reported that VGCF could usually be obtained by the decomposition of hydrocarbons using transition metal as catalyst at a temperature between 1000 °C and 1300 °C [28,29]. But Ajayan et al. [37] pointed out that carbon miro-trees could be deposited under extreme conditions (that is, using rapid heating and cooling cycles) without the help of catalyst particles. In this work, graphite particles which acted as a microwave absorber would result extreme high temperature points during MCVD process. That was different from the macro-temperature values detected by the infrared thermometer. Accordingly, the formation of VGCF in this work may
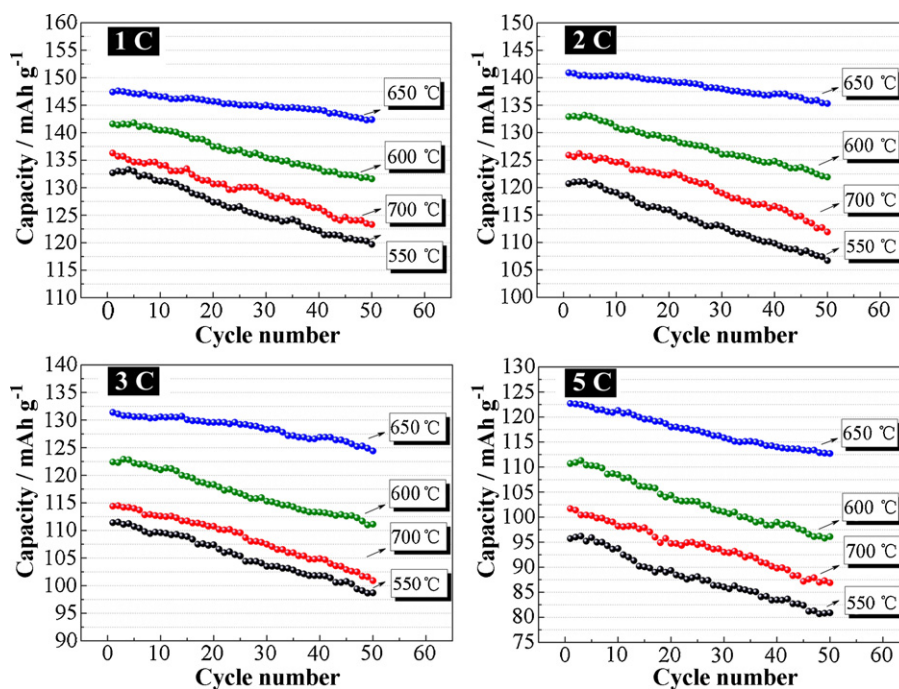

Fig. 5. Plots of discharge capacities of the samples prepared at different temperatures as a function of the cycle number in the first 50 cycles at the cutoff voltage of 2.5–4.2 V vs. Li/Li+ at different rates.
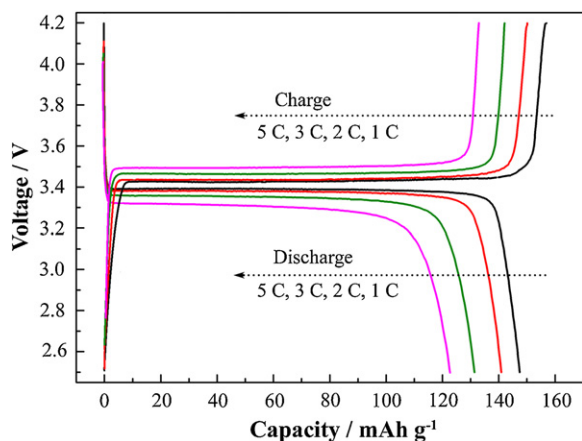
Fig. 6. Charge–discharge curves of the sample (obtained by MCVD process at 650 °C) measured with different rates at 25 °C.

Fig. 7. Impedance spectra of the samples prepared at different temperatures recorded with a frequency of between 10^5 Hz and 10^{-2} Hz.

result from the pyrolysis and deposition of propylene under special effect of microwave heating without any catalyst. This may also echo our previous study [34], though further research is still needed. In any case, a conductive network composed of VGCF, pyrolytic carbon film and graphite is formed in the as-prepared LiFePO$_4$-based composite through MCVD process. That is beneficial to facilitate faster charge transfer between the electrolyte and the LFP particles, which is supported by the electrochemical analyses discussed below.

Fig. 5 compares the rate capability and cycle performance of the samples obtained at different temperatures. The rate capability increased with the temperature increasing from 550 °C to 650 °C. The composite prepared at 650 °C exhibited the best rate capabilities. Its first discharge capacities varied from 147.5 mAh g^{-1} to 122.7 mAh g^{-1} with the discharge rates ranging from 1 C to 5 C (Fig. 6), and its capacity retention remained good at different rates.

According to the dissolution method, the carbon amount of all the as-prepared LiFePO$_4$-based samples is about 6 wt.%, and thus the total amount of both VGCF and pyrolytic carbon film in all electrodes is calculated to be approximately 1.9 wt.%. This indicated that the amount of carbon in the samples does not have an obvious change with the preparation temperature. The difference in the electrochemical performance shown in Fig. 5 may mainly result from the morphology and distribution of carbon materials in the electrodes but not the carbon amount.

Consequently, based on the above analyses, there are probably two reasons for the change in electrochemical performance. Firstly, with the temperature increasing from 550 °C to 650 °C, VGCF gradually forms a three-dimensional conductive network in the composite together with the pyrolytic carbon film and graphite. That would increase the electronic conductivity of the LiFePO$_4$-based composite cathode. Secondly, the forming VGCF network could improve the porosity of the composite cathode, which is beneficial to raise the contact area of the active materials and electrolyte. However, the rate capacity did not continue to be improved with the temperature further increasing. Instead, the composite synthesized at 700 °C had a much poor electrochemical performance than that prepared at 600 °C. This might be attributed to the LFP grain coarsening which increased the lithium ion diffusion length. Moreover, considering above XRD analyses, minor impurities were detected when the preparation temperature was up to 700 °C, which would also decrease the specific capacity to some extent.

Fig. 7 shows EIS analyses of the samples prepared at different temperatures. The EIS data were collected with a two electrode coin cell after activation (i.e., after subjecting the coin cell to two
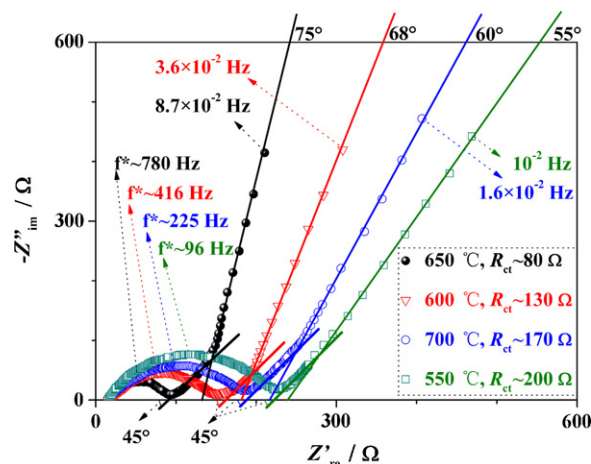
charge–discharge cycles). The initial activation was to suppress the lithium–electrolyte interfacial resistance arising from the passivating film formed on the lithium metal in contact with the electrolyte. The Nyquist plots of the composites exhibit a semicircle at high frequencies followed by a sloping line at medium frequencies. At very low frequencies the phase angle begins to increase due to the onset of finite length effects [38]. The characteristic frequency corresponding to charge transfer of different samples is 96 Hz (550 °C), 416 Hz (600 °C), 780 Hz (650 °C) and 225 Hz (700 °C), respectively. As such, the charge transfer resistance (R_{ct}, the diameter of the semicircle in Fig. 7) which is related to the electrochemical reaction at the electrode–electrolyte interface and particle–particle contact [39] is 200 Ω (550 °C), 130 Ω (600 °C), 80 Ω (650 °C) and 170 Ω (700 °C). This variation regularity is also supported by the changes in the rate capability and cycle performance of different samples as discussed above.

The exploitation of the Warburg domain (straight line at 45° at medium frequencies) which corresponds to the lithium diffusion into the host lattice (semi-infinite diffusion) allows determination of the kinetics of this limiting process through the calculation of the chemical diffusion coefficient D_{Li} with Eq. (1):

$$[D_{Li}]_{x_o} = \left(\frac{V_M}{\sqrt{2}FS} \left[\frac{dE}{dx} \right]_{x_o} \frac{1}{A} \right)^2 \tag{1}$$

where V_M is the molar volume (43.6 cm^3 mol^{-1}), F is the Faraday constant, S is the active surface area (cm^2) arbitrarily taken as the contact area between electrolyte and sample (2.5 cm^2), and A is the slope of the Warburg straight line ($Z_R = -Z_{Im} = A\omega^{-1/2}$). The coefficient of the samples prepared at different temperatures is around 10^{-13} to 10^{-14} cm^2 s^{-1}, which echoes the report by Franger et al. [40]. This is a low value for an insertion compound and it suggests that the electrochemical behavior of the composite is dependent on the current density, which has also been confirmed by the rate capability shown in Fig. 5 [40]. The higher the current applied, the lower the specific capacity obtained.

4. Conclusions

A novel microwave chemical vapor deposition approach has been shown to be an effective way to obtain LiFePO$_4$-based composite cathode materials in a short time (10 min). A three-dimensional conductive network provided by vapor-grown carbon fiber, pyrolytic carbon film and graphite can be formed in one step in virtue of this method. The electrochemical properties of the composite can be controlled by adjusting the preparation temperature

due to its regular effect on the structure and morphology of the as-prepared material. This work demonstrates a novel, energy efficient, rapid synthesis approach for preparing high-performance LFP cathodes for high power lithium ion batteries that are of interest for vehicle applications.

Acknowledgements

References

[1] C.H. Lu, P.V. Veh, W.T. Hsu, J. Alloys Compd. 476 (2009) 749.
[2] U. Dettlaff-Weglikowska, J. Yoshida, N. Sato, S. Roth, J. Electrochem. Soc. 158 (2011) A174.
[3] Q.S. Liu, L.H. Yu, H.H. Wang, J. Alloys Compd. 486 (2009) 886.
[4] Y.L. Ding, J.A. Xie, G.S. Gao, T.J. Zhu, H.M. Yu, X.B. Zhao, Adv. Funct. Mater. 21 (2011) 348.
[5] A. Manthiram, J.B. Goodenough, J. Solid State Chem. 71 (1987) 349.
[6] A.K. Padhi, K.S. Najundaswamy, J.B. Goodenough, J. Electrochem. Soc. 144 (1997) 1188.
[7] A.K. Padhi, K.S. Najundaswamy, C. Masquelier, S. Okada, J.B. Goodenough, J. Electrochem. Soc. 144 (1997) 1609.
[8] A.K. Padhi, K.S. Najundaswamy, C. Masquelier, J.B. Goodenough, J. Electrochem. Soc. 144 (1997) 2581.
[9] C. Wang, J. Hong, Electrochem. Solid-State Lett. 10 (2007) A65.
[10] K. Zaghib, A. Mauger, J.B. Goodenough, F. Gendron, C.M. Julien, Chem. Mater. 19 (2007) 3740.
[11] S.Y. Chung, J.T. Bloking, Y.M. Chiang, Nat. Mater. 1 (2002) 123.
[12] J.M. Yang, Y. Bai, C.B. Qing, W.F. Zhang, J. Alloys Compd. 509 (2011) 9010.
[13] G. Arnold, J. Garche, R. Hemmer, S. Strobele, C. Vogler, M. Wohlfahrt-Mehrens, J. Power Sources 121 (2003) 119–247.
[14] S.B. Lee, I.C. Jang, H.H. Lim, V. Aravindan, H.S. Kim, Y.S. Lee, J. Alloys Compd. 491 (2010) 668.
[15] I. Belharouak, C. Johnson, K. Amine, Electrochem. Commun. 7 (2005) 983.
[16] K. Zaghib, A. Mauger, F. Gendron, C.M. Julien, Chem. Mater. 20 (2008) 462.
[17] A. Yamada, S.C. Chung, K. Hinokuma, J. Electrochem. Soc. 148 (2001) A224.
[18] D. Choi, P.N. Kumta, J. Power Sources 163 (2007) 1064.
[19] K. Dokko, K. Shiraishi, K. Kanamura, J. Electrochem. Soc. 152 (2005) A2199.
[20] Y. Xia, W.K. Zhang, H. Huang, Y.P. Gan, J. Tian, X.Y. Tao, J. Power Sources 196 (2011) 5651.
[21] H. Yang, X.L. Wu, M.H. Cao, Y.G. Guo, J. Phys. Chem. C 113 (2009) 3345.
[22] G.T.K. Fey, Y.G. Chen, H.M. Kao, J. Power Sources 189 (2009) 169.
[23] S. Franger, F. Le Cras, C. Bourbon, H. Rouault, J. Power Sources 119 (2003) 252.
[24] C.M. Doherty, R.A. Caruso, B.M. Smarsly, C.J. Drummond, Chem. Mater. 21 (2009) 2895.
[25] M. Konarova, I. Taniguchi, J. Power Sources 195 (2010) 3661.
[26] M. Higuchi, K. Katayama, Yasuo Azuma, M. Yukawa, M. Suhara, J. Power Sources 119–121 (2003) 258.
[27] K.S. Park, J.T. Son, H.T. Chung, S.J. Kim, C.H. Lee, H.G. Kim, Electrochem. Commun. 5 (2003) 839.
[28] M. Endo, Y.A. Kim, T. Hayashi, K. Nishimura, T. Matusita, K. Miyashita, M.S. Dresselhaus, Carbon 39 (2001) 1287.
[29] H. Utsunomiya, T. Nakajima, Y. Ohzawa, Z. Mazej, B. Zemva, M. Endo, J. Power Sources 195 (2010) 6805.
[30] G.G. Tibbetts, Appl. Phys. Lett. 42 (1983) 666.
[31] C.C. Chen, M.H. Liu, J.M. Chen, 206th Meeting of the Electrochemical Society, Meeting Abstracts, Hawaii, 2004, p. 413.
[32] X.L. Li, F.Y. Kang, X.D. Bai, W.C. Shen, Electrochem. Commun. 9 (2007) 663.
[33] C. Sotowa, G. Origi, M. Takeuchi, Y. Nishimura, K. Takeuchi, I.Y. Jang, Y.J. Kim, T. Hayashi, Y.A. Kim, M. Endo, M.S. Dresselhaus, ChemSusChem 1 (2008) 911.
[34] J.Z. Zou, X.R. Zeng, X.B. Xiong, H.L. Tang, L. Li, Q. Liu, Z.Q. Li, Carbon 45 (2007) 828.
[35] D.J. Fu, X.R. Zeng, J.Z. Zou, H.X. Qian, X.H. Li, X.B. Xiong, Mater. Chem. Phys. 118 (2009) 501.
[36] X.R. Zeng, D.J. Fu, H.C. Sheng, S.H. Xie, X.H. Li, Q. Hu, J.Z. Zou, Physica E 42 (2010) 2103.
[37] P.M. Ajayan, J.M. Nugent, R.W. Siegel, B. Wei, Nature 404 (2000) 243.
[38] C. Ho, I.D. Raistrick, R.A. Huggins, J. Electrochem. Soc. 127 (1980) 343.
[39] Y.M. Choia, S.I. Pyun, Pyun Solid State Ionics 99 (1997) 173.
[40] S. Franger, F. Le Cras, C. Bourbon, H. Rouault, Electrochem. Solid State Lett. 5 (2002) A231.